PNAS RESEARCH ARTICLE | ECOLOGY

Urbanization and edge effects interact to drive mutualism breakdown and the rise of unstable pathogenic communities in forest soil

Chikae Tatsumi[a,b,c,1], Kathryn F. Atherton[a,d], Sarah M. Garvey[e], Emma Conrad-Rooney[a], Luca L. Morreale[e], Lucy R. Hutyra[e], Pamela H. Templer[a], and Jennifer M. Bhatnagar[a]

Edited by Mary Firestone, University of California, Berkeley, CA; received May 5, 2023; accepted July 21, 2023

Temperate forests are threatened by urbanization and fragmentation, with over 20% (118,300 km^2) of U.S. forest land projected to be subsumed by urban land development. We leveraged a unique, well-characterized urban-to-rural and forest edge-to-interior gradient to identify the combined impact of these two land use changes—urbanization and forest edge creation—on the soil microbial community in native remnant forests. We found evidence of mutualism breakdown between trees and their fungal root mutualists [ectomycorrhizal (ECM) fungi] with urbanization, where ECM fungi colonized fewer tree roots and had less connectivity in soil microbiome networks in urban forests compared to rural forests. However, urbanization did not reduce the relative abundance of ECM fungi in forest soils; instead, forest edges alone led to strong reductions in ECM fungal abundance. At forest edges, ECM fungi were replaced by plant and animal pathogens, as well as copiotrophic, xenobiotic-degrading, and nitrogen-cycling bacteria, including nitrifiers and denitrifiers. Urbanization and forest edges interacted to generate new "suites" of microbes, with urban interior forests harboring highly homogenized microbiomes, while edge forest microbiomes were more heterogeneous and less stable, showing increased vulnerability to low soil moisture. When scaled to the regional level, we found that forest soils are projected to harbor high abundances of fungal pathogens and denitrifying bacteria, even in rural areas, due to the widespread existence of forest edges. Our results highlight the potential for soil microbiome dysfunction—including increased greenhouse gas production—in temperate forest regions that are subsumed by urban expansion, both now and in the future.

ectomycorrhizal fungi | urbanization | forest edge | microbial function

Significance

Urbanization and forest edge creation are increasingly altering Earth's ecosystems, yet the effects on soil microbiomes—which are crucial for plant health and climate regulation—remain unclear. Our data indicate that these two combined, compounding stressors reshape the soil microbiome of forests in ways that reduced the function of tree symbionts, increased plant and animal pathogen loads, and enhanced the potential for denitrification. By identifying the specific environmental stressors that lead to these microbiome shifts, our analysis can inform urban development and forest management plans to mitigate impacts on the soil microbiome to sustain environmental quality and the ecosystem services that remnant native forests provide to society in the coming decades.

The world's forests are being rapidly urbanized and fragmented by land development (1, 2), with more than 70% located within 1 km of a forest edge (3), especially in temperate regions which contain 52% more edge forest area than tropical regions (4). However, we are still in the early stages of understanding how urbanization and forest edge creation impact some of a forest's most important ecological communities. Soil microbes are critical regulators of carbon (C) loss and sequestration in forests, accelerating tree mortality by acting as pathogens, sustaining aboveground forest productivity by increasing nutrient availability for plants (5), or storing C belowground in stable microbial products (6). Recent studies show dramatic shifts in the composition and activity of soil microbiomes with urbanization (7–10) and at forest edges (11). Urban forests are situated near developed cities, while forest edges are characterized by a zone on one side that lacks trees due to deforestation. However, the combined, compounding impacts of these two intense land development activities on soil microbial communities are unclear. Urbanization, fragmentation, and forest edge creation are expanding worldwide, with the loss of interior forests occurring up to seven times faster than the loss of edge forests in the temperate zone (12). At the same time, society has increased its reliance on temperate forests in urban and rural areas for recreational, esthetic, and health benefits (13, 14). Understanding the form and function of microbial communities within fragmented urban forests will become increasingly critical as we depend on them more heavily to sustain environmental quality and human well-being in the coming decades.

The multiple, interacting environmental stressors of urbanization and forest edge effects may be particularly detrimental to microbial mutualists of plants, similar to the negative impact of environmental stress on plant–animal mutualisms (15) and microbial symbionts of animals (16). Urban areas have higher ambient air temperatures, greenhouse gas concentrations (e.g., carbon dioxide; CO_2), nitrogen (N) loads (e.g., ammonium and nitrate deposition), and ambient pollutants (e.g., particulate matter and ozone; O_3) relative to rural areas (17–21). Especially sensitive to these conditions are fungal symbionts of tree

Author contributions: C.T., S.M.G., L.R.H., P.H.T., and J.M.B. designed research; C.T., K.F.A., S.M.G., E.C.-R., and J.M.B. performed research; C.T., K.F.A., L.L.M., and J.M.B. analyzed data; and C.T., K.F.A., E.C.-R., L.L.M., and J.M.B. wrote the paper.

The authors declare no competing interest.

This article is a PNAS Direct Submission.

[1]To whom correspondence may be addressed. Email: ctatsumi@bu.edu.

This article contains supporting information online at https://www.pnas.org/lookup/suppl/doi:10.1073/pnas.2307519120/-/DCSupplemental.

Published August 29, 2023.

roots (e.g., ectomycorrhizal (ECM) fungi), which provide nutrients (such as N) to host trees in return for plant C (5). ECM fungi often decline when soil N availability rises or when plant photosynthesis slows due to land cover change or pollutant exposure, potentially because plants allocate less C belowground (22–24). Forest edges can exacerbate urban stressors, as they experience higher air and soil temperatures (25) and higher nutrient and pollutant deposition compared to forest interiors (26). ECM fungi are critical mediators of ecosystem energy and element flows: they can funnel up to 50% of plant C belowground and provide up to 80% of plant N, while also providing pathogen protection to trees (27), ultimately controlling forest productivity to a degree that impacts atmospheric CO_2 levels and the stability of the global climate (28). If ECM fungi decline at forest edges, then urban edge forests—which comprise a rapidly increasing fraction of the world's forests (1, 3)—may have a dramatically lower capacity for C and nutrient sequestration than their rural, interior forest counterparts (29–31), especially if trees become more vulnerable to pathogens.

Another way in which urbanization and forest edges may impact the soil microbiome is by increasing the vulnerability of soil communities to both abrupt and long-term environmental stress, similar to edge effects on forest trees (4, 32, 33). Evidence is accumulating that there is a growth-stress tolerance trade-off in microorganisms (34–37), similar to that in macroorganisms (38, 39), such that a fast-growing soil community may have a lower tolerance to environmental stress. If fast-growing microbes are favored at forest edges, they may have lower stress tolerance and experience higher turnover, or instability, over time (40). The effect would be exacerbated if soil microbiomes become more homogeneous with urbanization, as seen in plant and animal communities (41, 42). Urbanization can create unique environments that favor the growth of certain species (41–43), leading some to suggest the existence of an "urban suite" of soil microbes (44), similar to groups of plants often found in urban settings (45). However, urbanization can also generate high spatial habitat and community heterogeneity (46, 47), potentially accelerating evolutionary dynamics (48, 49), so it is unclear what the overall impact of urbanization and forest edges have on microbial community structure if urban forest communities can withstand additional environmental stressors from edge effects, and what the role of these communities is in the health and functioning of forests.

We hypothesized that urbanization and forest edges interact to reduce ECM abundance in soils, shifting soil microbial communities toward more pathogenic and copiotrophic taxa, particularly at urban forest edges. We also expected urbanization and forest edges to homogenize soil microbial communities, selecting for communities with fewer associations between taxa and making soil communities more vulnerable to environmental stress, which could explain changes in soil N cycling and C storage observed at urban forest edges (33, 50, 51). To test these hypotheses, we examined soil microbial community composition in the Urban New England (UNE) study (33, 50, 51), which includes a series of eight fragmented, ECM-dominated temperate forest sites along a 120-km urban-to-rural gradient in the State of Massachusetts (MA). At UNE, duplicate sampling points are located along a 90-m transect from the forest edge to the forest interior at each site (8 sites × 5 distances from the edge × 2 sampling points = 80 sampling points in total, Fig. 1 and *SI Appendix*, Table S1). We paired three years of data (2018, 2019, and 2021) on soil microbial community composition measured at each UNE sampling point (227 samples in total) with soil biogeochemistry (e.g., full elemental analysis, soil respiration rates, and rates of net ammonification and nitrification) and physiochemistry (e.g., pH, temperature, moisture) data from the same soil samples, as well as data on root biomass, ECM colonization rates, and plant density and community composition. We tested the impact of urbanization (measured as the distance from an urban center (Boston Common in Boston,

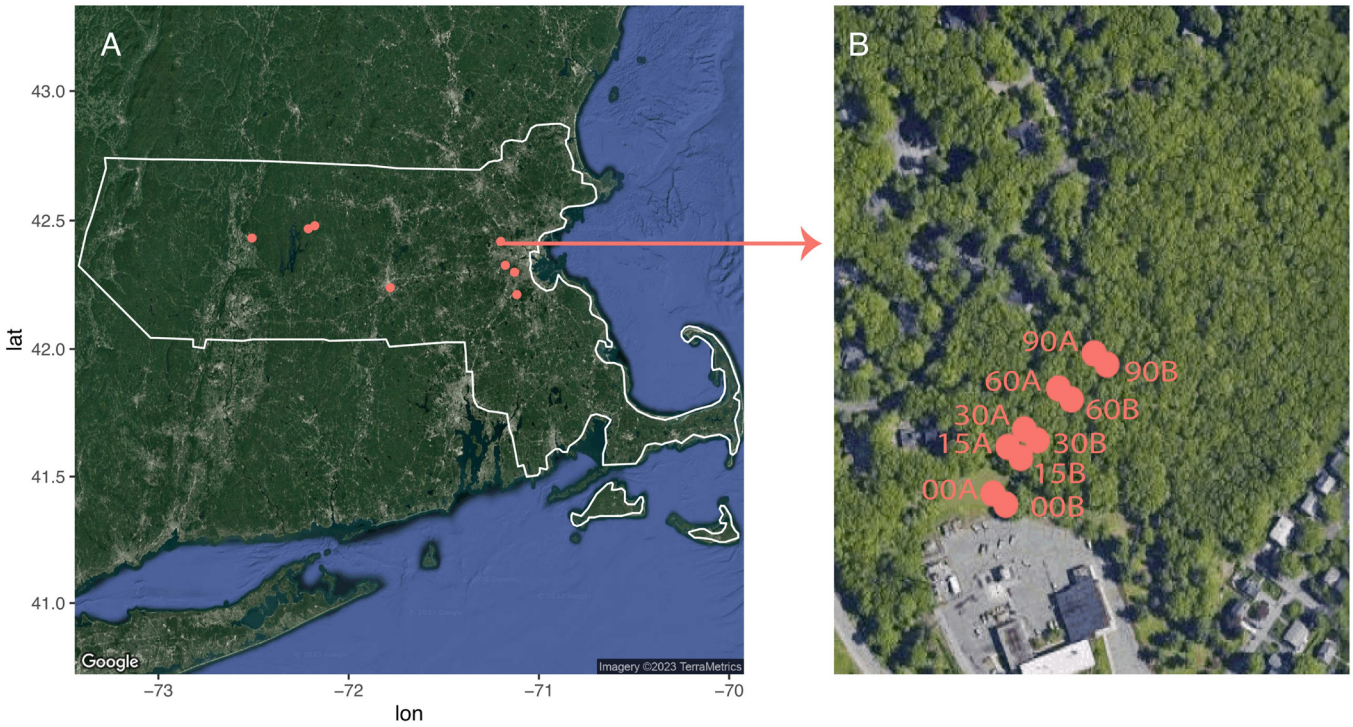

Fig. 1. Map of sampling regime and sampling locations across the UNE study system. Circles represent individual sampling locations mapped on Google Map images. (*A*) Individual sampling sites are shown on a map of the state of Massachusetts. (*B*) Individual sampling locations (replicates *A* and *B*) within a sampling site (Sutherland Woods) along the 0–90 m distance from forest edge transect within an individual 100-m × 100-m plot are shown. lat, latitude; lon, longitude.

MA) and forest edges [classified as the distance from the forest edge (33, 51)] on soil microbial communities using a combination of linear regression models that accounted for spatial autocorrelation in community composition (*SI Appendix*, Fig. S1), differential abundance analyses, and covariance network analyses. To understand the potential roles of microbial groups in soil C and N cycling, we also looked for relationships between the abundance of microbial C and N-cycling functional groups, C and N and total soil respiration rates (51), N transformations (33), and C stocks (50). Additionally, we scaled the results of our analyses to the state level, leveraging soil microbiome data we generated for each of the ECM-dominated USDA FIA forest types in MA. In MA, which is one of the most densely populated and densely forested states in the United States, forests cover 60% of the land surface but are heavily fragmented due to urban sprawl (52), where over two-thirds of the population currently live (53). Increases in temperature at the forest edge compared to the forest interior are comparable to the amount of warming this region experienced between 1900 and 1999 due to climate change (54).

Results and Discussion

In contrast to our expectations, neither urbanization nor its interaction with forest edges reduced ECM fungal abundance in soils of remnant, native forests. Instead, forest edges alone had striking negative effects on ECM fungi: ECM fungi declined precipitously in soil at the edges of both urban and rural forests (Fig. 2*A*) despite a similar relative density of ECM trees and similar root biomass at forest edges compared to forest interiors (*SI Appendix*, Fig. S2). These results indicate that recent reports of reduced ECM fungal abundance in urban soils worldwide (9) could be explained in part by edge effects on fragmented urban landscapes. Loss of ECM fungi was correlated with an increase in fungal and bacterial diversity in soils at forest edges (*SI Appendix*, Fig. S3) due to an increase in pathogenic microbes (Fig. 2 *B* and *C* and *SI Appendix*, Table S2), xenobiotics-degrading and copiotrophic bacteria, as well as nitrate-producing and consuming bacteria (*SI Appendix*, Table S2 and Fig. S3). This shift in soil microbiome composition from ECM fungi to nitrate-cycling bacteria was mirrored by increased nitrification rates at forest edges (*SI Appendix*, Fig. S4) (33) and parallels results from other studies showing that nitrifying bacteria may compete with ECM fungi for ammonium (55). Denitrifying bacteria also showed high abundance at the forest edge, indicating a high potential for forest edges to release nitrogenous greenhouse gases (e.g., N_2O and NO_2) that may accelerate atmospheric warming and feedback to increase drought stress in forest edges. Interestingly, animal pathogen abundance was also high at forest edges (Fig. 2*B* and *SI Appendix*, Table S2), as was the abundance of dung-saprotrophic fungi (*SI Appendix*, Table S2), suggesting a greater influence of animals on the soil microbiome at both urban and rural forest edges.

Despite high relative abundances of ECM fungi in urban forest soils, we found evidence of tree–ECM mutualism breakdown under urbanization: urban trees had lower ECM colonization rates on roots (Fig. 2*D*), despite higher ECM tree and root abundance (*SI Appendix*, Fig. S2) and increased plant N uptake (leaf N concentration, *SI Appendix*, Fig. S4 and Table S2) relative to rural trees. This result is consistent with one other study that quantified ECM colonization of trees planted in urban street tree pits vs. rural forests (56), which found lower ECM colonization of trees in street pits. High rates of net N mineralization in urban sites (33) might explain this phenomenon, as we found that experimental N addition at rural forests reduced the ECM colonization rate to levels close to those found in urban forests (*SI Appendix*, Fig. S5). High levels of inorganic N in soil have an overwhelmingly negative effect on tree–ECM symbioses (57), suggesting that the benefit of strong

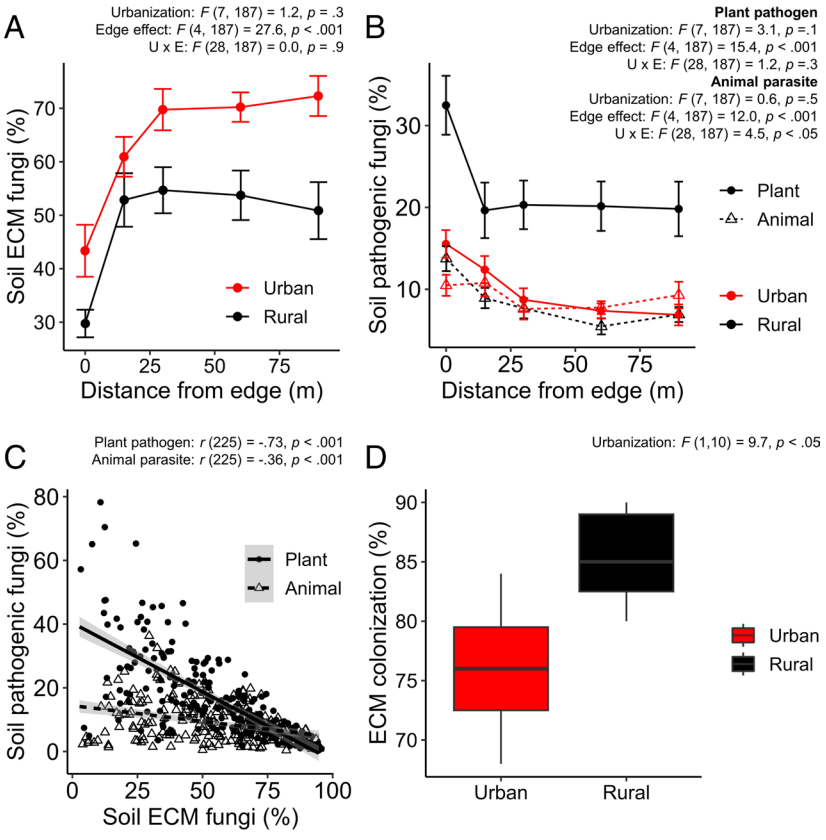

Fig. 2. Relationships between urbanization and forest edges and key plant- and animal-associated soil microbes. The relationship between distance from the forest edge and the relative abundances of (*A*) ECM fungi and (*B*) pathogenic fungi calculated from FungalTraits are shown. (*C*) ECM fungi are anticorrelated with pathogenic fungi in the soil, including plant and animal pathogens. Differences in (*D*) ECM colonization of oak trees between urban sites and rural sites illustrate the breakdown of tree–ECM mutualisms with urbanization. ANOVA results for the linear mixed-effect models testing for relationships with urbanization (negative distance from Boston), edge effects (negative distance from edge), and their interactions (U × E) are shown for ECM fungi (*A*), fungal pathogens (*B*), and ECM colonization (*D*). Correlation test results for the fungal group are shown (*C*). The error bar of the line graphs shows the SE.

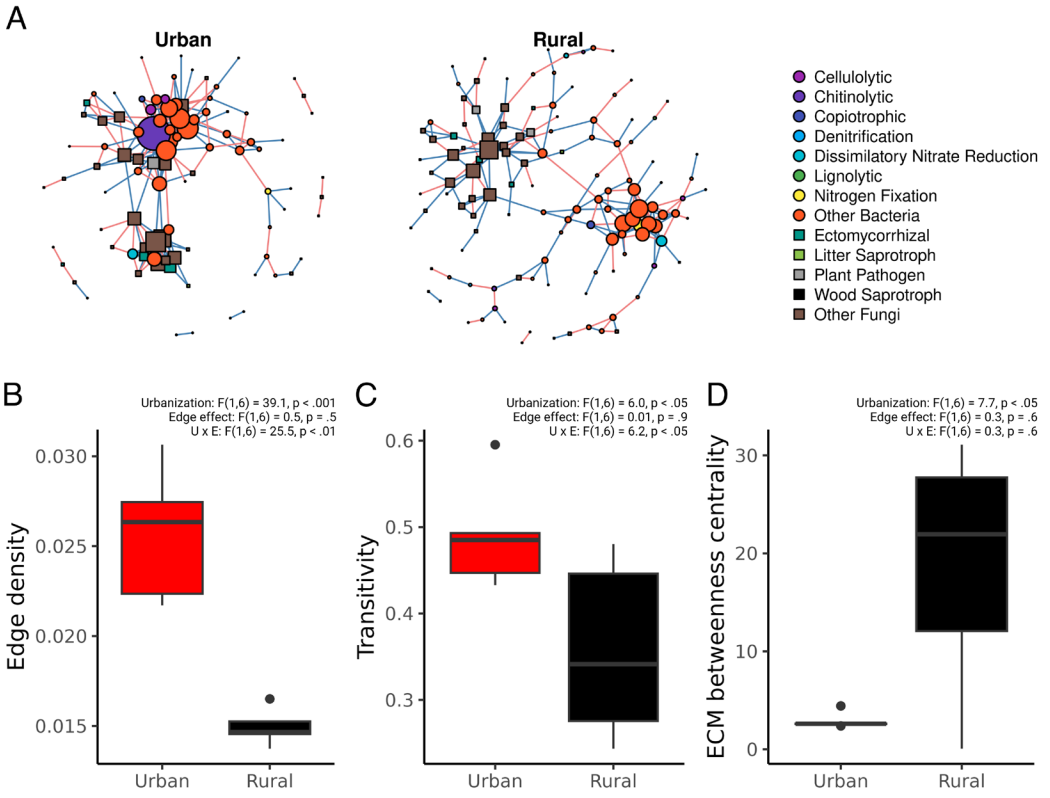

Fig. 3. (*A*) Networks of urban and rural forests. Circles represent in-house database-based bacterial functional groups and squares represent FungalTraits-based fungal functional groups. Sizes of circles and squares represent the degree, or number of connections, of the taxa. Positive associations are colored blue and negative associations are colored red. ANOVA results for the linear mixed-effect models testing for relationships with urbanization (negative distance from Boston), edge effects (negative distance from edge), and their interactions (U × E) are shown for network metrics edge density (*B*), transitivity, or "cliqueness" (*C*), and ECM betweenness centrality, or network importance (*D*).

tree–ECM mutualisms under the high temperature and drought stress in urban systems might not outweigh the benefit of reducing C allocation to symbionts under high soil N availability.

Tree–ECM mutualism breakdown, combined with additional unique environmental conditions in urban forests, changed community structure and species connectivity in the soil microbiome. In contrast to our expectations, network analysis revealed that urban soil microbiomes were highly connected, with taxa clustering into densely connected "cliques" (Fig. 3 *A* and *B*) that indicate strong covariance of taxa in response to environmental conditions (58). Interestingly, ECM fungi were less central in urban soil community networks than in rural networks (Fig. 3*D*). Instead, the most connected taxa in urban soil networks were other, less well-studied bacteria and fungi (Fig. 3*A*). This switch from soil microbiomes connected by tree symbionts to ones potentially structured by the activity of free-living saprotrophs suggests that the combination of higher soil temperatures and lower ECM activity may be the major impact of urbanization on microbiome

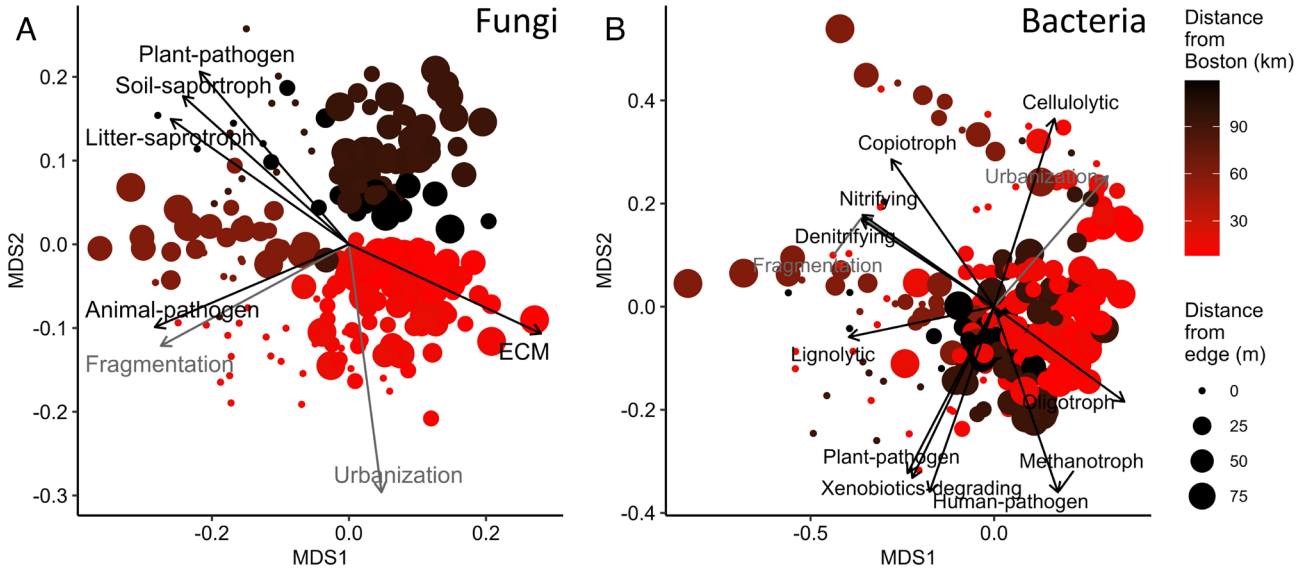

Fig. 4. Community composition of (*A*) fungi and (*B*) bacteria, including suites of urban/rural and edge/interior forest soil microbes. Point color and size represent the distance from Boston (km) and the distance from the forest edge (m), respectively. Differential abundance of microbial groups across suites was tested using the vegan::envfit function (70), and significant groups are shown on each plot (70). 1) All the fungal functional groups, 2) nitrifying and denitrifying bacteria, 3) pathogenic and xenobiotic-degrading bacteria, and 4) all the other bacterial functional groups referred to 1) FungalTraits, 2) amoA- and nosZ- targeting qPCR, 3) PICRUSt2, and 4) in-house database, respectively.

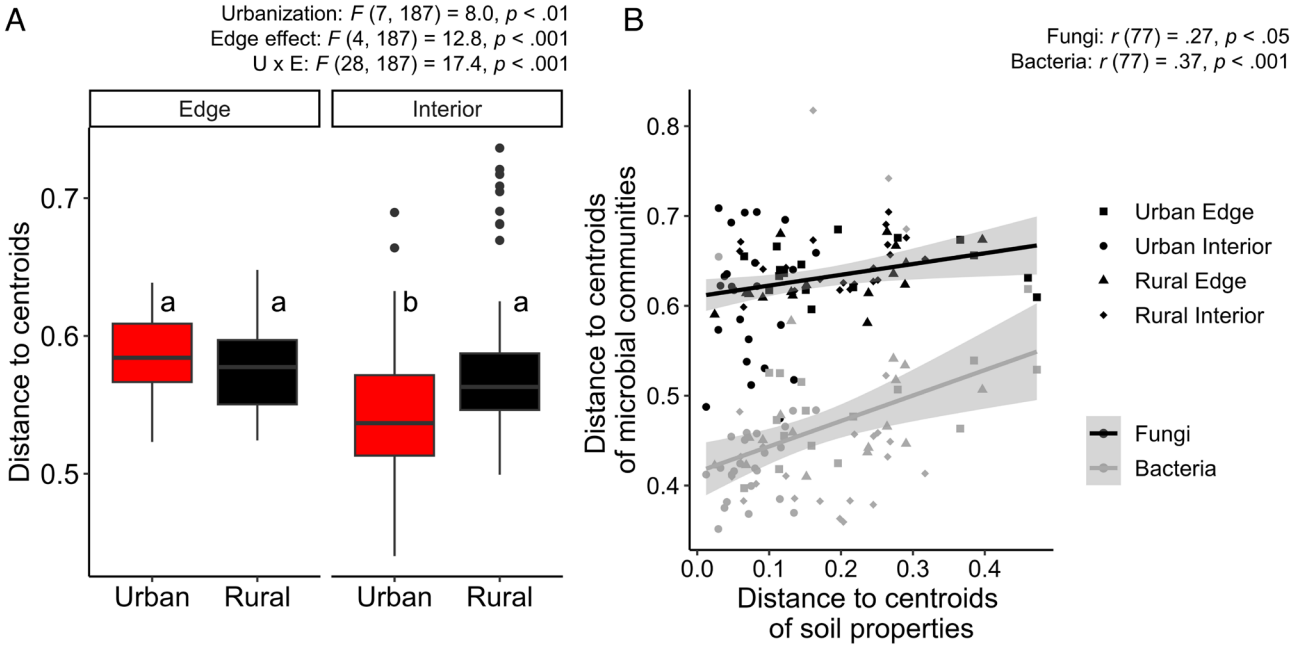

Fig. 5. (*A*) Homogenization (measured as distance to centroids) of soil microbial (both fungal and bacterial) communities in each location (urban edge, urban interior, rural edge, rural interior), and (*B*) the relationships between homogenization of soil properties and soil microbial communities. The result of ANOVA for the linear mixed-effect model for urbanization, edge effects, and their interactions (U × E) and the results of Tukey's multiple comparison tests (*A*), and the correlation coefficients (*B*) are shown.

structure and metabolism. Microbial network connectivity was positively correlated with soil and foliar C content (*SI Appendix*, Fig. S4), consistent with other studies (59, 60), providing evidence of a relationship between C storage and ecosystem complexity (61) across urban-to-rural gradients.

Together, urbanization and forest edges interacted to generate suites of soil microbes that characterized each forest type that was phylogenetically diverse (*SI Appendix*, Fig. S6) but functionally constrained. For example, urban forest interiors were characterized by ECM fungi and cellulolytic, nitrate/nitrite-reducing, and methanotroph bacteria, while urban edges were defined by plant pathogens and nitrifying taxa (Fig. 4 and *SI Appendix*, Fig. S7). Consistent with our expectations, urban forest soil communities were more homogeneous than rural forests, but only in forest interiors (Fig. 5*A*). This phenomenon corresponded to the homogenization of soil properties (soil temperature, moisture, pH,

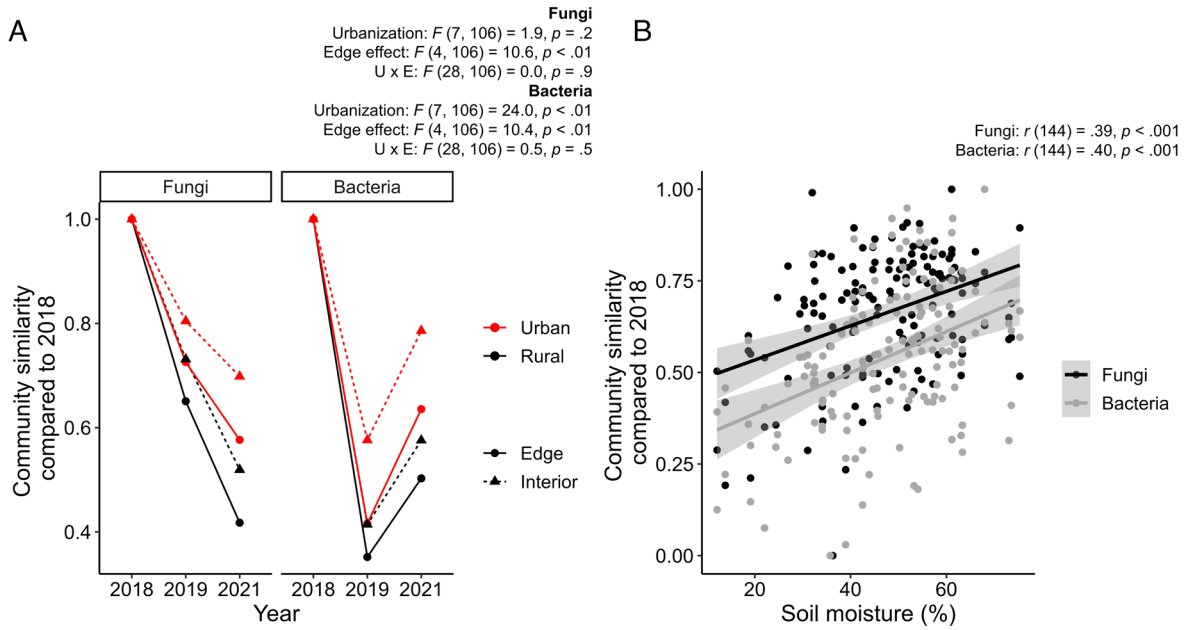

Fig. 6. Community instability across urban/rural and edge/interior forest soils (*A*) and community vulnerability to drought stress across sites (*B*). Instability was calculated as community similarity (calculated as Aitchison distance) compared to the 1st year (2018), of which community was the baseline of the comparison (*A*), and vulnerability to drought stress was calculated as the relationship between community instability and soil moisture (*B*). The result of ANOVA for the linear mixed-effect model for urbanization, edge effects, and their interactions (U × E) is shown (*A*), and the correlation coefficients for fungal and bacterial community instability are shown (*B*).

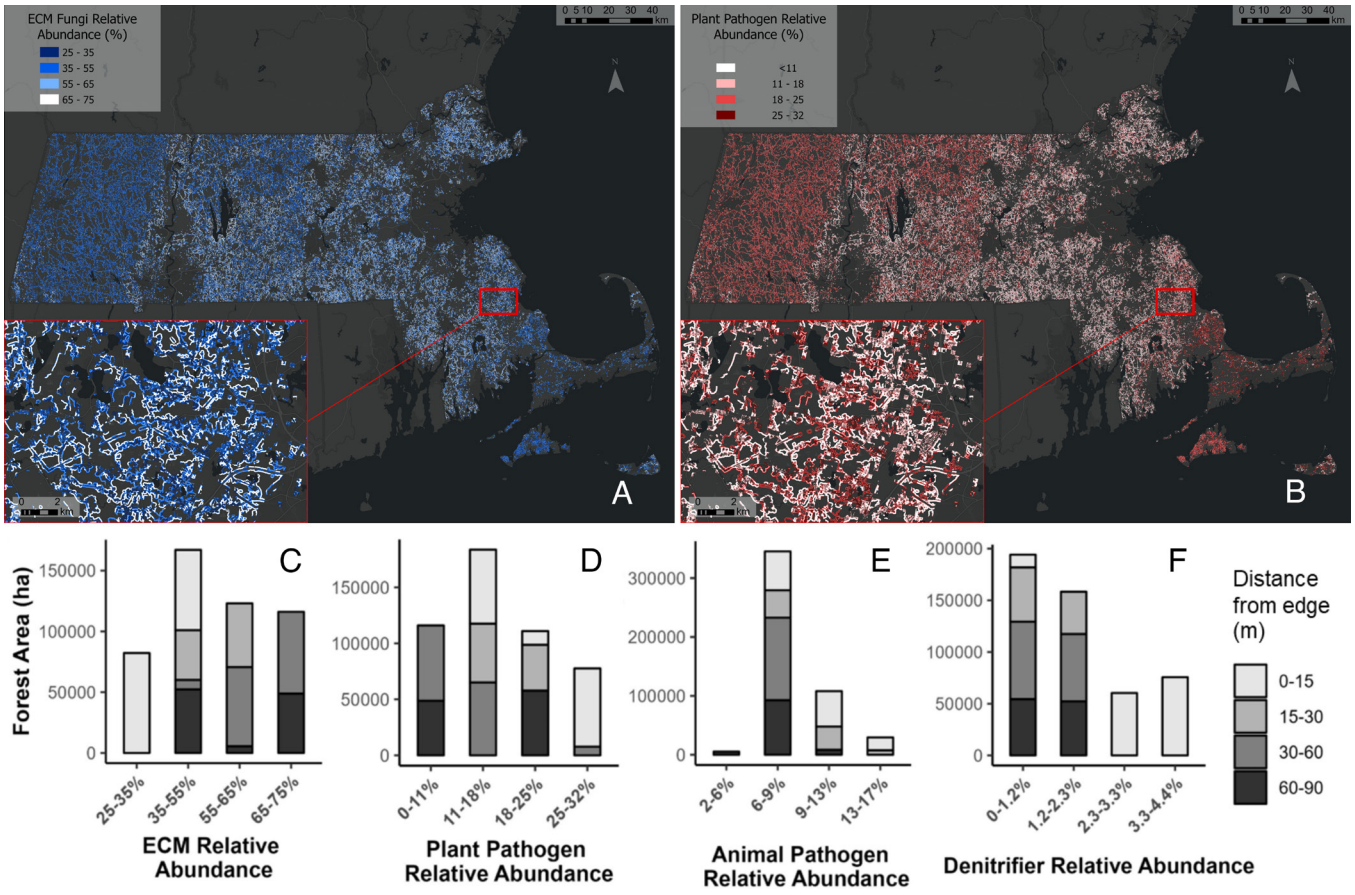

Fig. 7. Projected abundances of microbial groups in ECM-dominated forests in the mixed rural and urban landscape across the state of Massachusetts. Forest type groups at UNE field sites were matched with US Forest Service forest types, then relative abundances of key fungal [ECM fungi (*A* and *C*), plant pathogens (*B* and *D*), and animal pathogens (*E*)] and bacterial denitrifying groups (*F*) calculated for each UNE plot were projected across interior and edge forest areas within the state. The amount of forest areas (in ha) that contain a certain fraction (%) of microbial functional groups is shown (*C*–*F*). Edge forest was categorized as forest area bordered by non-forest in distance-from-edge bins (15, 30, 60, and 90 m). The abundances of fungal functional groups and denitrifying bacteria were calculated based on FungalTraits categorization of ITS amplicon sequence data and qPCR of the nosZ gene in soil DNA extracts, respectively.

organic matter content, ammonium content, and nitrate content) in the interiors of urban forests (Fig. 5*B*), similar to other studies that have found urbanization homogenizes the physical environment (62) and contributes to biotic homogenization of plants and animals (41, 43). By contrast, forest edge microbiomes were more heterogeneous and tended to change more dramatically over time—or be less stable—than at the forest interior (Fig. 6*A*). Instability of both bacterial and fungal communities was linked to increased vulnerability to low soil moisture (Fig. 6*B*), which is most severe at the forest edge (50). Soil microbial vulnerability to drought has been hypothesized for the last decade (63) and our data provide the evidence that this is a key way in which urbanization and forest edges impact the soil microbiome. Interestingly, bacteria are less stable than fungi and more sensitive to low soil moisture at forest edges (Fig. 6*B*), potentially because they are more dependent on water for dispersal (64, 65). Forest edges also experience larger fluctuations of soil water content than interiors, because of high light intensity in edge habitats (66), a process that is known to change microbial community composition (67, 68). In addition, because ECM fungi can connect microbiome members by providing plant C and N (69), a loss of ECM fungi could also partially explain community instability at forest edges (Fig. 6*A*).

When we scale the change in forest soil microbiomes with urbanization and edge creation across ECM-dominated forests for the state of MA, we project unexpectedly high regional loads of plant and animal pathogens (Fig. 7). While ECM fungi comprise >55% of the soil fungal community for forests in most of this territory, plant pathogens make up over a quarter of the soil fungal community in over 77,000 ha of forest area. This phenomenon is associated with widespread forest edges, resulting in strikingly high projected levels of fungal pathogens in the rural, typically regarded as pristine, western part of the state. The loss of tree symbionts and the rise of pathogenic microbiomes in forests could explain reduced tree growth at the edges of temperate forests that experience extreme heat stress (32). In addition to fungal pathogens, we project extremely high levels of denitrifying bacteria across the state: over 130,000 Ha of forest across the state harbors more than double the relative abundance of denitrifiers found in soils of intact, interior rural forests (Fig. 7), indicating potential for greater N-based greenhouse gas emissions from soil than previously expected.

Conclusion

Arguably one of the greatest—and most poorly understood—threats to temperate forests is edge creation through land clearing and development. Northern temperate hardwood forests are already the most urbanized and fragmented forest type in the world and have the highest likelihood of becoming more fragmented and urbanized in the coming decades (1, 2). Our study suggests that urbanization and edge effects from this land development have

strong negative impacts on tree symbionts and their role as keystone taxa in soil microbial communities. In contrast to our expectations, urban forest soils can be dominated by ECM fungi, if there is a high percentage of ECM trees in the forest stand. However, higher soil N availability—driven by increasingly warmer soil temperatures and high N pollution in urban areas—may threaten tree–ECM symbioses and dramatically change urban forest composition in the near future (71). Our observation that soil at forest edges has fewer ECM fungi and increases in pathogenic and N-cycling microbes indicates that where ECM trees decline, we may see additional increases in pathogen and denitrifier loads beyond what we now project for the region.

Materials and Methods

Study System and Sample Collection. The Urban New England (UNE) study consists of eight mid-successional, temperate, deciduous forest sites spanning an urban-to-rural gradient in Massachusetts (*SI Appendix*, Fig. S1 and Table S1). Here, we defined the urbanization gradient as the distance from an urban core (33), where Park Street Station in Boston represented the urban end of the gradient, and Leverett, MA represents the rural end. Microbial communities are more similar when grouped based on the distance from the urban center (Boston), rather than by other well-known urbanization indicators, such as impervious surface area (Fig. 4 and *SI Appendix*, Fig. S8) (72). Each of 8 sites at UNE consists of 5 plots that are 10 m × 20 m in area and are located at 0, 15, 30, 60, and 90 m from the forest edge (40 plots in total). The climate at these sites is humid continental with warm summers (mean monthly temperatures of 18.6 °C to 21.7 °C) and cold, snowy winters (−4.3 °C to −0.1 °C), and 1,100–1,300 mm of precipitation distributed evenly throughout the year (NOAA 2021). Dominant tree species are mostly ECM-associates such as red oak (*Quercus rubra*), white pine (*Pinus strobus*), sweet birch (*Betula lenta*), although some plots have a high abundance of red maple (*Acer rubrum*), and sugar maple (*Acer saccharum*). The total tree basal area per plot ranged from 10.5 to 94.0 m^2 ha^{-1} (*SI Appendix*, Table S1). Additional site details are available in Garvey et al. (51) and Caron et al. (33).

Organic horizon soils (0.8–9.7 cm depth) at UNE were collected in August 2018, July 2019, and July 2021. Organic horizon soils contain the vast majority of soil microbial activity, including N mineralization (33) and extracellular enzyme activities (50). Two replicate soil samples were collected in each plot at the same time and location as soil respiration and temperature measurements were taken from PVC respiration collars installed on the forest floor (51) (227 samples in total; 40 plots × 2 replicates × 3 sampling years). We omitted 1 and 12 samples from 2018 and 2021, respectively, because of plot accessibility. Soil samples were kept on ice during same-day transport back to the laboratory and stored at 4 °C until processing within 72 h of sampling. Soils were sieved through a 2-mm sieve and then a subsample was stored in a −80 °C freezer until DNA extraction. Additional fresh soil subsamples were used to measure soil physicochemical properties, including gravimetric moisture content, pH, organic matter concentration, C and N content, and ammonium and nitrate content (33, 51). Net N mineralization and nitrification rates, root ECM colonization rate, and foliar C and N content measured at UNE (33, 50, 51) were also included in the analysis. Details for all biogeochemical assays and plant measurements can be found in *SI Appendix, Supplementary Methods*.

Soil DNA Extraction, Quantitative PCR, Fungal/Bacterial Amplicon Sequencing, and Bioinformatics.

DNA extraction. Total soil DNA was extracted from approximately 0.25 g of soil using the DNeasy PowerSoil HTP 96 Kit (QIAGEN, Hilden, Germany). Two technical replicates were extracted from one soil sample, resulting in 454 extracts in total ({8 sites × 5 plots × 2 biological replicates × 3 sampling years − 13 samples} × 2 technical replicates). Extracts were stored frozen at −80 °C until further analysis.

Amplicon sequencing. The two DNA extractions (technical replicates) from each soil sample were pooled to better represent soil microbiome diversity (73). Modified versions of the primer set fITS7 and ITS4 were used for fungi, amplifying the ITS2 region of rDNA (74, 75) and modified versions of the primer set 515f and 806r, which target the v4 16S region of rDNA, were used for bacteria (76). Primers contained both the Illumina adapter and individual sample indexes (77, 78). Amplicon sequencing was conducted on the pooled DNA extract per sample (227 samples in total). Amplicons were checked by agarose gel electrophoresis, then cleaned using the Just-a-Plate 96 PCR Purification and Normalization Kit (Charm Biotech, MO) and quantified using the Qubit HS-dsDNA kit (Invitrogen, Carlsbad, CA). 16S and ITS amplicons for each sample were mixed at equimolar concentrations. Both 16S and ITS amplicons for 80 samples at maximum were combined into a single library for sequencing, generating six libraries in total. Each library was subject to 250 base pair (bp) paired-end sequencing on Illumina MiSeq run at the TUFTS Genome Sequencing Core facility. Sequence data were deposited in the Sequence Read Archive at NCBI under accession number DRA015736.

Bioinformatics was performed in the R software environment (version 4.0.0), where the R package dada2 was used for sequence quality control, paired-end assembly, identification of amplicon sequence variants (ASVs), and taxonomy assignment (79). Taxonomy was assigned to ASVs using the naive Bayesian classifier method (80) in combination with the UNITE database (v. 7.2) (81) as the reference for fungal ITS ASVs and the SILVA database (release 138.1) (82) as the reference for bacterial ASVs. To assign taxa to functional guilds, fungal ASVs were searched against the FungalTraits database (83), and bacterial genera were searched against an in-house functional database created based on the presence of genes coding for enzymes in specific biochemical pathways (copiotroph, oligotroph, cellulolytic, ligninolytic, methanotroph, chitinolytic, assimilatory nitrite-reducing, dissimilatory-nitrite reducing, assimilatory nitrate-reducing, dissimilatory nitrate-reducing) (84, 85). PICRUSt2 (86) was used for predicting the bacterial xenobiotic-degrading and pathogenic gene abundances for each sample based on KEGG Orthology (KO) (87) annotations. Suites of bacteria and fungi were calculated for each location group (i.e., Urban edge, Urban interior, Rural edge, and Rural interior) using indicator species analysis (88).

Quantitative PCR (qPCR). Due to the small population sizes of certain fungal and bacterial functional groups (such as arbuscular mycorrhizal fungi, N-fixing bacteria, nitrifying bacteria, and denitrifying bacteria) within the community, their abundance could not be accurately determined based on amplicon sequencing. Therefore, we conducted a qPCR analysis specifically targeting these groups. AM fungi (18S rDNA), N-fixing bacteria (nifH), nitrifying bacteria (amoA), and denitrifying bacteria (nosZ) genes were quantified by qPCR following published protocols with several modifications (89–92). In addition, to facilitate the comparison between fungal and bacterial amplicon sequencing-based relative abundances, total fungal and bacterial gene abundances were quantified using the same primer sets employed in amplicon sequencing [fITS7/ITS4 for fungi (74, 75), and 515f/806r for bacteria (76)]. A detailed description of the qPCR conditions is included in *SI Appendix, Supplementary Methods*.

Covariance network analysis. We constructed covariance networks for soil microbial communities at each distance from edge (0, 15, 30, 60, 90 m from forest edge) in urban and rural forests, resulting in 10 different soil microbiome networks. Samples from the same plot for urban and rural forests (i.e., urban forest 0 m plots, urban forest 15 m plots, rural forest 0 m plots, etc.) across all sampling years were combined to construct a network (2 samples per plot × 4 forests per forest type × 3 sampling years = 24 samples per network). For network construction, we collapsed fungal and bacterial amplicon sequence counts to the genus level and normalized each genus by total fungal and bacterial abundance based on qPCR. Functional groups of the genus were detected using the FungalTratis database and the in-house database for fungi and bacteria, respectively. Abundance tables were filtered (*SI Appendix, Supplementary Methods*) and networks were constructed using the SpiecEasi package of R (93) (parameters are described in *SI Appendix, Supplementary Methods*). Networks were analyzed for measures of connectivity, overall topological structure, and taxon importance using the igraph package of R (94).

Scaling to the State of MA. To explore the implications of our findings over a mixed rural and urban landscape, we scaled our results across the state of MA. We first applied forest compositional groups defined by the US Forest Service (Forest Inventory & Analysis User's Manual Appendix D) to categorize each of our study sites based on their species composition. UNE sites were classified as white/red/jack pine (Code 100), oak/pine (Code 400), pine/hickory (Code 500), or maple/beech/birch (Code 800). We used a one-meter resolution land-cover map developed by the Massachusetts Bureau of Geographic Information (available at https://www.mass.gov/info-details/massgis-data-2016-land-coverland-use) to categorize forest area bordered by nonforest into distance-from-edge bins [15, 30, 60, and 90 m;

sensu Reinmann et al. (32)]. We then categorized the US Forest Service forest types within this high-resolution land-cover map using a 250-m resolution forest composition map (95). We selected only forested areas of the same forest type as the UNE study sites, then estimated the relative abundances of microbial community constituents in MA based on patterns of distance from edge and forest composition.

Statistical Analysis. Prior to statistical analyses, data were normalized in multiple ways, depending on the data type. For qPCR, data were normalized via logarithmic function. For amplicon sequence data, we normalized ASV counts across samples using the rarefaction, which lowers the false discovery rate of ASVs when samples vary >10-fold in sequencing depth (96). ASV counts per sample were rarefied by equalizing final read numbers to 18,028 reads for fungal communities and 11,384 reads for bacterial communities using random pick-up based on the minimum read number. We found that normalization by ANCOM-BC (97) and rarefaction produced similar results across analyses (*SI Appendix*, Table S3), so we report results of taxonomic and functional group analyses with rarefied data, allowing us to include rare taxa in the analysis.

To explore relationships between urbanization, edge effects, and the soil microbiome, we used distance from Boston and distance from the edge, as well as their interaction, as the fixed independent variables for all statistical models. To account for repeated sampling at individual locations, UNE sampling site was included as a random variable in each model (33). Shannon's alpha diversity for the whole fungal and bacterial community was calculated by the vegan package (70) in R. For community instability, Aitchison's dissimilarities (98) were calculated on the unrarefied ASV tables where a value of "1" was added to all values. We then converted Aitchison's dissimilarities to similarities ranging from one to zero using the following algorithm: 1 − ((value − min)/(max − min)). To test for urbanization and edge effects on community homogenization, the distance to centroids was calculated in each location group (i.e., Urban edge, Urban interior, Rural edge, and Rural interior). Urban and rural site designations were based on distance from Boston (33) and the edge included 0–15 m, while the interior included a 30–90 m distance from the forest edge. Urban and edge effects on microbial community were calculated using a linear mixed-effect model (LMM). ANOVA test for LMMs was run for values, standardized by the scale function in R, using the lme4 and lmerTest packages (99, 100) in R. Community differences among soil samples were visualized by nonmetric multidimensional scaling (NMDS) of community structure based on the Bray-Curtis dissimilarity index using the metaMDS function in the vegan package (70) of R. The envfit function was used to illustrate significant correlations between fungal or bacterial functional groups and community dissimilarity among soil samples.

We measured the relationships between environmental factors, urbanization, and edge effects using an LMM. At UNE, urbanization was significantly positively correlated with soil temperature, and net N mineralization rate, but significantly negatively correlated with total tree basal area (*SI Appendix*, Table S2*B*). Forest edges were significantly positively correlated with soil pH, soil nitrate content, net nitrification rate, total tree basal area, and foliar C: N ratio, but significantly negatively correlated with soil moisture, SOM concentration, soil net N mineralization rate, and soil respiration rate (*SI Appendix*, Table S2*B*). To see the significant correlations between microbial functional groups and environmental variables, *Pearson*'s correlation test was used. We set the level of significance at 5% for all statistical tests. The codes are available on GitHub (https://github.com/Chikae-Tatsumi/UNE).

Data, Materials, and Software Availability. Raw sequence data are available under DDBJ/NCBI BioProject PRJDB15313 (101).

ACKNOWLEDGMENTS. We thank the Arnold Arboretum of Harvard University, Harvard Forest, Massachusetts Department of Conservation & Recreation, Massachusetts Department of Environmental Protection, the Massachusetts Department of Transportation, Massachusetts Audubon Society, National Grid, Cities of Newton and Lexington, MA, and all landowners for allowing research on their properties. We are also grateful for the assistance in the laboratory, fields, or data analysis, or the helpful comments on earlier drafts of this manuscript from members of Bhatnagar, Templer, and Hutyra Labs, as well as Jerry Melillo, John Hobbie, Maggie Anderson, Talia Michaud, Takuro Ogura, Jonathan Gewirtzman, Stephen Caron, Nahuel Policelli, Corinne Vietorisz, Michael Silverstein, and Zoey Werbin. This study was financially supported in part by NSF NRT DGE 1735087; Grant-in-Aid for JSPS Research Fellow (Grant Nos. 17J07686 and 20J00656), Oversea Challenge Program for Young Researcher (Grant No. 201980107) to C.T.; United States Department of Agriculture and National Institute of Food and Agriculture grant to Templer and Hutyra (USDA NIFA 67003-26615), DOE BER award DE-SC0020403, a Patricia McLellan Leavitt Research Award, a startup fund from Boston University and Boston University's internal Peter Paul Professorship fund to J.M.B.; and the Boston University Microbiome Initiative Accelerator Program to J.M.B. and K.F.A. The genomics work conducted by the U.S. Department of Energy Joint Genome Institute, a DOE Office of Science User Facility, is supported by the Office of Science of the U.S. Department of Energy under Contract No. DE- AC02-05CH11231.

Author affiliations: [a]Department of Biology, Boston University, Boston, MA 02215; [b]Graduate School of Agriculture, Kyoto University, Kyoto 606-8502, Japan; [c]Research Faculty of Agriculture, Hokkaido University, Hokkaido 060-0809, Japan; [d]Bioinformatics Graduate Program, Boston University, Boston, MA 02215; and [e]Department of Earth and Environment, Boston University, Boston, MA 02215

1. D. Nowak, J. Walton, Projected urban growth (2000–2050) and its estimated impact on the US Forest Resource. *J. For.* **103**, 383–389 (2005).
2. S. Angel, J. Parent, D. L. Civco, A. Blei, D. Potere, The dimensions of global urban expansion: Estimates and projections for all countries, 2000–2050. *Prog. Plan.* **75**, 53–107 (2011).
3. N. M. Haddad *et al.*, Habitat fragmentation and its lasting impact on Earth's ecosystems. *Sci. Adv.* **1**, e1500052 (2015).
4. L. L. Morreale, J. R. Thompson, X. Tang, A. B. Reinmann, L. R. Hutyra, Elevated growth and biomass along temperate forest edges. *Nat. Commun.* **12**, 7181 (2021).
5. Sally E. Smith, David J. Read, *Mycorrhizal Symbiosis* (Academic Press, 2010).
6. I. Kögel-Knabner *et al.*, Organo-mineral associations in temperate soils: Integrating biology, mineralogy, and organic matter chemistry. *J. Plant Nutr. Soil Sci.* **171**, 61–82 (2008).
7. K. S. Ramirez *et al.*, Biogeographic patterns in below-ground diversity in New York City's Central Park are similar to those observed globally. *Proc. R. Soc. B Biol. Sci.* **281**, 20141988 (2014).
8. N. Hui *et al.*, Ectomycorrhizal fungal communities in urban parks are similar to those in natural forests but shaped by vegetation and park age. *Appl. Environ. Microbiol.* **83**, e01797-17 (2017).
9. D. J. Epp Schmidt *et al.*, Urbanization erodes ectomycorrhizal fungal diversity and may cause microbial communities to converge. *Nat. Ecol. Evol.* **1**, 0123 (2017).
10. K. Kiesewetter, M. Afkhami, Microbiome-mediated effects of habitat fragmentation on native plant performance. *New Phytol.* **232**, 1823–1838 (2021).
11. T. Ramsfield *et al.*, Distance from the forest edge influences soil fungal communities colonizing a reclaimed soil borrow site in boreal mixedwood forest. *Forests* **11**, 427 (2020).
12. USDA Forest Service, *Future of America's Forests and Rangelands: Update to the 2010 Resources Planning Act Assessment* (U.S. Department of Agriculture, Forest Service, Washington Office, 2016).
13. R. B. Primack, C. Terry, New social trails made during the pandemic increase fragmentation of an urban protected area. *Biol. Conserv.* **255**, 108993 (2021).
14. A. J. Miller-Rushing *et al.*, COVID-19 pandemic impacts on conservation research, management, and public engagement in US National Parks. *Biol. Conserv.* **257**, 109038 (2021).
15. A. Magrach, W. F. Laurance, A. R. Larrinaga, L. Santamaria, Meta-analysis of the effects of forest fragmentation on interspecific interactions. *Conserv. Biol.* **28**, 1342–1348 (2014).
16. J. J. Wernegreen, Mutualism meltdown in insects: Bacteria constrain thermal adaptation. *Curr. Opin. Microbiol.* **15**, 255–262 (2012).
17. G. M. Lovett *et al.*, Atmospheric deposition to oak forests along an urban—rural gradient. *Environ. Sci. Technol.* **34**, 4294–4300 (2000).
18. L. H. Ziska, J. A. Bunce, E. W. Goins, Characterization of an urban-rural CO_2/temperature gradient and associated changes in initial plant productivity during secondary succession. *Oecologia* **139**, 454–458 (2004).
19. K. George, L. H. Ziska, J. A. Bunce, B. Quebedeaux, Elevated atmospheric CO_2 concentration and temperature across an urban–rural transect. *Atmos. Environ.* **41**, 7654–7665 (2007).
20. E. Paoletti, A. De Marco, D. C. S. Beddows, R. M. Harrison, W. J. Manning, Ozone levels in European and USA cities are increasing more than at rural sites, while peak values are decreasing. *Environ. Pollut.* **192**, 295–299 (2014).
21. Y. Fang *et al.*, Nitrogen deposition and forest nitrogen cycling along an urban-rural transect in southern China. *Glob. Change Biol.* **17**, 872–885 (2011).
22. E. W. Morrison *et al.*, Chronic nitrogen additions fundamentally restructure the soil fungal community in a temperate forest. *Fungal Ecol.* **23**, 48–57 (2016).
23. A. Corrales, B. L. Turner, L. Tedersoo, S. Anslan, J. W. Dalling, Nitrogen addition alters ectomycorrhizal fungal communities and soil enzyme activities in a tropical montane forest. *Fungal Ecol.* **27**, 14–23 (2017).
24. M.-M. Kytöviita, D. Le Thiec, P. Dizengremel, Elevated CO_2 and ozone reduce nitrogen acquisition by Pinus halepensis from its mycorrhizal symbiont. *Physiol. Plant.* **111**, 305–312 (2008).
25. G. R. Matlack, Microenvironment variation within and among forest edge sites in the eastern United States. *Biol. Conserv.* **66**, 185–194 (1993).
26. K. C. Weathers, M. L. Cadenasso, S. T. A. Pickett, Forest Edges as nutrient and pollutant concentrators: Potential synergisms between fragmentation, forest canopies, and the atmosphere. *Conserv. Biol.* **15**, 1506–1514 (2001).
27. M. G. A. Heijden, F. M. Martin, M. Selosse, I. R. Sanders, Mycorrhizal ecology and evolution: The past, the present, and the future. *New Phytol.* **205**, 1406–1423 (2015).
28. M. Shi, J. B. Fisher, E. R. Brzostek, R. P. Phillips, Carbon cost of plant nitrogen acquisition: Global carbon cycle impact from an improved plant nitrogen cycle in the Community Land Model. *Glob. Change Biol.* **22**, 1299–1314 (2016).
29. C. W. Fernandez, J. A. Langley, S. Chapman, M. L. McCormack, R. T. Koide, The decomposition of ectomycorrhizal fungal necromass. *Soil Biol. Biochem.* **93**, 38–49 (2016).

30. K. E. Clemmensen *et al.*, Roots and associated fungi drive long-term carbon sequestration in boreal forest. *Science* **339**, 1615–1618 (2013).
31. C. E. Siletti, C. A. Zeiner, J. M. Bhatnagar, Distributions of fungal melanin across species and soils. *Soil Biol. Biochem.* **113**, 285–293 (2017).
32. A. B. Reinmann, I. A. Smith, J. R. Thompson, L. R. Hutyra, Urbanization and fragmentation mediate temperate forest carbon cycle response to climate. *Environ. Res. Lett.* **15**, 114036 (2020).
33. Stephen Caron *et al.*, Urbanization and fragmentation have opposing effects on soil nitrogen availability in temperate forest ecosystems. *Glob. Change Biol.* **29**, 2156–2171 (2023).
34. K. L. Herr *et al.*, Exopolysaccharide production in Caulobacter crescentus: A resource allocation trade-off between protection and proliferation. *PLoS ONE* **13**, e0190371 (2018).
35. J. E. Hallsworth, Stress-free microbes lack vitality. *Fungal Biol.* **122**, 379–385 (2018).
36. A. A. Malik *et al.*, Defining trait-based microbial strategies with consequences for soil carbon cycling under climate change. *ISME J.* **14**, 1–9 (2020).
37. M. A. Anthony, T. W. Crowther, D. S. Maynard, J. van den Hoogen, C. Averill, Distinct assembly processes and microbial communities constrain soil organic carbon formation. *One Earth* **2**, 349–360 (2020).
38. P. V. A. Fine *et al.*, The growth-defense trade-off and habitat specialization by plants in Amazonian forests. *Ecology* **87**, S150–S162 (2006).
39. T. Albrecht, C. T. Argueso, Should I fight or should I grow now? The role of cytokinins in plant growth and immunity and in the growth–defence trade-off. *Ann. Bot.* **119**, 725–735 (2016).
40. J. J. Faith *et al.*, The long-term stability of the human gut microbiota. *Science* **341**, 1237439 (2013).
41. M. L. McKinney, Urbanization as a major cause of biotic homogenization. *Biol. Conserv.* **127**, 247–260 (2006).
42. R. B. Blair, "Birds and Butterflies Along Urban Gradients in Two Ecoregions of the United States: Is Urbanization Creating a Homogeneous Fauna?" in *Biotic Homogenization*, J.L. Lockwood, M.L. McKinney, Eds. (Springer, US, 2001), pp. 33–56.
43. D. A. Holway, A. V. Suarez, Homogenization of ant communities in mediterranean California: The effects of urbanization and invasion. *Biol. Conserv.* **127**, 319–326 (2006).
44. A. S. Karpati, S. N. Handel, J. Dighton, T. R. Horton, Quercus rubra-associated ectomycorrhizal fungal communities of disturbed urban sites and mature forests. *Mycorrhiza* **21**, 537–547 (2011).
45. Peter Del Tredici, *Wild Urban Plants of the Northeast: A Field Guide* (Cornell University Press, 2020).
46. J. Niemelä, Ecology and urban planning. *Biodivers. Conserv.* **8**, 119–131 (1999).
47. T. Scholier *et al.*, Urban forest soils harbour distinct and more diverse communities of bacteria and fungi compared to less disturbed forest soils. *Mol. Ecol.* **32**, 504–517 (2022).
48. M. Schilthuizen, *Darwin Comes to Town: How the Urban Jungle Drives Evolution* (Picador, 2019).
49. M. T. J. Johnson, J. Munshi-South, Evolution of life in urban environments. *Science* **358**, eaam8327 (2017).
50. Sarah Garvey, Pamela H. Templer, Jennifer M. Bhatnagar, Lucy Hutyra, Soils at the temperate forest edge: An investigation of soil characteristics and carbon dynamics. *Sci. Total Environ.* **891**, 164320 (2023).
51. S. M. Garvey, P. H. Templer, E. A. Pierce, A. B. Reinmann, L. R. Hutyra, Diverging patterns at the forest edge: Soil respiration dynamics of fragmented forests in urban and rural areas. *Glob. Change Biol.* **28**, 3094–3109 (2022).
52. B. J. Butler, *Forests of Massachusetts, 2017* (U.S. Department of Agriculture, Forest Service, Northern Research Station, 2018).
53. Census profile: Boston-Cambridge-Newton, MA-NH Metro Area. *Census Report* (2021). http://censusreporter.org/profiles/31000US14460-boston-cambridge-newton-ma-nh-metro-area/
54. K. Hayhoe *et al.*, Past and future changes in climate and hydrological indicators in the US Northeast. *Clim. Dyn.* **28**, 381–407 (2007).
55. C. Tatsumi, T. Taniguchi, S. Du, N. Yamanaka, R. Tateno, Soil nitrogen cycling is determined by the competition between mycorrhiza and ammonia-oxidizing prokaryotes. *Ecology* **101**, e02963 (2020).
56. L. D. Bainard, J. N. Klironomos, A. M. Gordon, The mycorrhizal status and colonization of 26 tree species growing in urban and rural environments. *Mycorrhiza* **21**, 91–96 (2011).
57. E. K. Stuart, K. L. Plett, Digging Deeper, In search of the mechanisms of carbon and nitrogen exchange in ectomycorrhizal symbioses. *Front. Plant Sci.* **10**, 1658 (2020).
58. K. Faust, Open challenges for microbial network construction and analysis. *ISME J.* **15**, 3111–3118 (2021).
59. J. Guo *et al.*, Soil fungal assemblage complexity is dependent on soil fertility and dominated by deterministic processes. *New Phytol.* **226**, 232–243 (2020).
60. L. Qiu *et al.*, Erosion reduces soil microbial diversity, network complexity and multifunctionality. *ISME J.* **15**, 2474–2489 (2021).
61. D. Moreno-Mateos *et al.*, The long-term restoration of ecosystem complexity. *Nat. Ecol. Evol.* **4**, 676–685 (2020).
62. P. M. Groffman *et al.*, Ecological homogenization of urban USA. *Front. Ecol. Environ.* **12**, 74–81 (2014).
63. F. T. de Vries, A. Shade, Controls on soil microbial community stability under climate change. *Front. Microbiol.* **4**, 265 (2013).
64. A. Kravchenko *et al.*, Relationships between intra-aggregate pore structures and distributions of *Escherichia coli* within soil macro-aggregates. *Appl. Soil Ecol.* **63**, 134–142 (2013).
65. J. K. Carson *et al.*, Low pore connectivity increases bacterial diversity in soil. *Appl. Environ. Microbiol.* **76**, 3936–3942 (2010).
66. A. B. Reinmann, L. R. Hutyra, Edge effects enhance carbon uptake and its vulnerability to climate change in temperate broadleaf forests. *Proc. Natl. Acad. Sci. U.S.A.* **114**, 107–112 (2017).
67. M.-V. Dinh, A. Guhr, A. R. Weig, E. Matzner, Drying and rewetting of forest floors: Dynamics of soluble phosphorus, microbial biomass-phosphorus, and the composition of microbial communities. *Biol. Fertil. Soils* **54**, 761–768 (2018).
68. D. Liu *et al.*, Response of microbial communities and their metabolic functions to drying-rewetting stress in a temperate forest soil. *Microorganisms* **7**, 129 (2019).
69. S. Gorka *et al.*, Rapid transfer of plant photosynthates to soil bacteria via ectomycorrhizal hyphae and its interaction with nitrogen availability. *Front. Microbiol.* **10**, 168 (2019).
70. Jari Oksanen *et al.*, *Vegan: Community Ecology Package. R* (2020).
71. C. Averill, M. C. Dietze, J. M. Bhatnagar, Continental-scale nitrogen pollution is shifting forest mycorrhizal associations and soil carbon stocks. *Glob. Change Biol.* **24**, 4544–4553 (2018).
72. P. Rao, L. R. Hutyra, S. M. Raciti, A. C. Finzi, Field and remotely sensed measures of soil and vegetation carbon and nitrogen across an urbanization gradient in the Boston metropolitan area. *Urban Ecosyst.* **16**, 593–616 (2013).
73. L. M. Feinstein, W. J. Sul, C. B. Blackwood, Assessment of bias associated with incomplete extraction of microbial DNA from soil. *Appl. Environ. Microbiol.* **75**, 5428–5433 (2009).
74. K. Ihrmark *et al.*, New primers to amplify the fungal ITS2 region–Evaluation by 454-sequencing of artificial and natural communities. *FEMS Microbiol. Ecol.* **82**, 666–677 (2012).
75. T. J. White, T. Bruns, S. Lee, J. W. Taylor "Amplification and direct sequencing of fungal ribosomal RNA genes for phylogenetics" in *PCR Protocols: A Guide to Methods and Applications*, M.A. Innis, D.H. Gelfand, J.J. Sninsky, T.J. White, Eds. (Academic press, 1990), pp. 315–322.
76. J. G. Caporaso *et al.*, Global patterns of 16S rRNA diversity at a depth of millions of sequences per sample. *Proc. Natl. Acad. Sci. U.S.A.* **108**, 4516–4522 (2011).
77. M. A. Anthony, S. D. Frey, K. A. Stinson, Fungal community homogenization, shift in dominant trophic guild, and appearance of novel taxa with biotic invasion. *Ecosphere* **8**, e01951 (2017).
78. J. M. Bhatnagar, K. G. Peay, K. K. Treseder, Litter chemistry influences decomposition through activity of specific microbial functional guilds. *Ecol. Monogr.* **88**, 429–444 (2018).
79. B. J. Callahan *et al.*, DADA2: High-resolution sample inference from Illumina amplicon data. *Nat. Methods* **13**, 581–583 (2016).
80. Q. Wang, G. M. Garrity, J. M. Tiedje, J. R. Cole, Naïve Bayesian classifier for rapid assignment of rRNA sequences into the new bacterial taxonomy. *Appl. Environ. Microbiol.* **73**, 5261–5267 (2007).
81. R. H. Nilsson *et al.*, The UNITE database for molecular identification of fungi: Handling dark taxa and parallel taxonomic classifications. *Nucleic Acids Res.* **47**, D259–D264 (2019).
82. C. Quast *et al.*, The SILVA ribosomal RNA gene database project: Improved data processing and web-based tools. *Nucleic Acids Res.* **41**, D590–D596 (2012).
83. S. Põlme *et al.*, FungalTraits: A user-friendly traits database of fungi and fungus-like stramenopiles. *Fungal Divers.* **105**, 1–16 (2020).
84. R. Berlemont, A. C. Martiny, Phylogenetic distribution of potential cellulases in bacteria. *Appl. Environ. Microbiol.* **79**, 1545–1554 (2013).
85. M. B. N. Albright, B. Timalsina, J. B. H. Martiny, J. Dunbar, Comparative genomics of nitrogen cycling pathways in Bacteria and Archaea. *Microb. Ecol.* **77**, 597–606 (2019).
86. Gavin M. Douglas *et al.*, PICRUSt2 for prediction of metagenome functions. *Nat. Biotechnol.* **38**, 669–673 (2020).
87. M. Kanehisa, Y. Sato, M. Kawashima, M. Furumichi, M. Tanabe, KEGG as a reference resource for gene and protein annotation. *Nucleic Acids Res.* **44**, D457–D462 (2016).
88. M. D. Cáceres, P. Legendre, Associations between species and groups of sites: Indices and statistical inference. *Ecology* **90**, 3566–3574 (2009).
89. C. R. Hewins, S. R. Carrino-Kyker, D. J. Burke, Seasonal variation in mycorrhizal fungi colonizing roots of *Allium tricoccum* (wild leek) in a mature mixed hardwood forest. *Mycorrhiza* **25**, 469–483 (2015).
90. D. J. Levy-Booth, C. E. Prescott, S. J. Grayston, Microbial functional genes involved in nitrogen fixation, nitrification and denitrification in forest ecosystems. *Soil Biol. Biochem.* **75**, 11–25 (2014).
91. M. Saifuddin, J. M. Bhatnagar, R. P. Phillips, A. C. Finzi, Ectomycorrhizal fungi are associated with reduced nitrogen cycling rates in temperate forest soils without corresponding trends in bacterial functional groups. *Oecologia* **196**, 863–875 (2021).
92. T. Helgason, T. J. Daniell, R. Husband, A. H. Fitter, J. P. W. Young, Ploughing up the wood-wide web? *Nature* **394**, 431–431 (1998).
93. Z. D. Kurtz *et al.*, Sparse and compositionally robust inference of microbial ecological networks. *PLoS Comput. Biol.* **11**, e1004226 (2015).
94. G. Csárdi, T. Nepusz *The igraph Software Package for Complex Network Research.Complex System 1695*, 1–9 (2006).
95. B. Ruefenacht *et al.*, Conterminous U.S. and Alaska forest type mapping using forest inventory and analysis data. *Photogramm. Eng. Remote Sens.* **74**, 1379–1388 (2008).
96. S. Weiss *et al.*, Normalization and microbial differential abundance strategies depend upon data characteristics. *Microbiome* **5**, 27 (2017).
97. H. Lin, S. D. Peddada, Analysis of compositions of microbiomes with bias correction. *Nat. Commun.* **11**, 3514 (2020).
98. J. Aitchison, The statistical analysis of compositional data. *J. R. Stat. Soc. Ser. B Methodol.* **44**, 139–177 (1982).
99. D. Bates, M. Mächler, B. Bolker, S. Walker, Fitting linear mixed-effects models using lme4. *J. Stat. Softw.* **67**, 1–48 (2015).
100. A. Kuznetsova, P. B. Brockhoff, R. H. B. Christensen, **lmerTest** Package: Tests in linear mixed effects models. *J. Stat. Softw.* **82**, 1–26 (2017).
101. C. Tatsumi *et al.*, Urbanization and edge effects interact to drive mutualism breakdown and the rise of unstable pathogenic communities in forest soil. National Library of Medicine Bioproject PRJDB15313. https://www.ncbi.nlm.nih.gov/bioproject/PRJDB15313. Accessed 14 August 2023.